



Characterization of unary precursor-based geopolymer bonded composite developed from ground granulated blast slag and lignocellulosic material residues

H. O. Olayiwola¹ · S. O. Amiandamhen² · M. Meincken¹ · L. Tyhoda¹ 

Received: 1 June 2021 / Accepted: 7 December 2021 / Published online: 5 January 2022
© The Author(s), under exclusive licence to Springer-Verlag GmbH Germany, part of Springer Nature 2022

Abstract

The excellent properties of geopolymer composites and their ability to be synthesized from various industrial waste streams make them promising green binders in wood-based composite manufacturing. The study characterized 100% slag unary precursor-based geopolymers reinforced with lignocellulosic material residue. The residue included sugarcane bagasse (SCB), Port Jackson (*Acacia saligna*) and Black wattle (*Acacia mearnsii*). The production process was established based on a mixed factorial design using Statistica 13.3. The factors considered included a curing pattern at 2 levels, sodium hydroxide concentration at 3 levels and lignocellulose material at 3 levels. Other parameters, such as precursor-activator ratio and sodium hydroxide-silicate ratio were constant. Statistical analysis revealed that curing temperature and sodium hydroxide concentration had a significant effect on the board properties and the addition of lignocellulose material improved the flexural strength. Curing at 40 °C influenced the reaction kinetics, enhanced microstructural properties, and produced a dense geopolymeric matrix which resulted in improved physical and mechanical properties. However, increasing the sodium hydroxide concentration beyond 6 M caused efflorescence and deteriorated the mechanical property of *A. mearnsii* and bagasse boards. Partial degradation of the fibres was confirmed by Fourier transform infrared spectroscopy and thermogravimetric analysis, but the degraded products did not inhibit geopolymer setting. Scanning electron microscopy indicated a uniform board structure surrounded with micro crystals of calcium silicate hydrate (C–S–H). *A. saligna* boards produced with 6 M NaOH and cured at 40 °C met the technical specification of cement-bonded particleboards for outdoor applications according to the British standard EN 634–2.

1 Introduction

Several industrial operations, such as coal power plants and iron smelters are based on a linear model of “take, make, dispose” leading to depletion of natural resources (Sariatli 2017). The residues are usually landfilled, posing serious environmental challenges. However, the bulk of these residues can serve as resource material to produce secondary products. Fly ash and slag derived from coal burning and iron smelting, respectively have been used as precursor materials in the development of geopolymer binders, which can

be an alternative, green substitute for cement and concrete products in different applications (Provis and Van Deventer 2014), including inorganic-bonded wood composites (Korniejenko et al. 2015; Olayiwola et al. 2021). Geopolymer binder is developed by alkali activation of naturally occurring or industrial residues rich in amorphous aluminosilicate compounds (Alomayri 2017). The wood-cement industry is well established, but the intensive energy requirements during cement production and its impact on the environment are overshadowing the excellent properties of cement-bonded products. About 60–130 kg of combustible material and 110 kWh of electricity are required to produce 1 ton of cement (Lamas et al. 2013), emitting an equivalent 1.1 ton of CO₂ into the atmosphere (Aiken et al. 2017). The energy requirements of cement production and its accompanying effects on the population and the environment has resulted in intensified efforts at finding alternative green binders for wood composite manufacturing. Geopolymers derived from industrial residues do not only have comparable properties

✉ L. Tyhoda
ltyhoda@sun.ac.za

¹ Department of Forest and Wood Science, Stellenbosch University, Stellenbosch, South Africa

² Department of Forestry and Wood Technology, Linnaeus University, Växjö, Sweden

to concrete products, but they also have a reduced energy requirement in their production with lower impact on the environment (Komnitsas 2011).

The inherent chemical or mineral characteristics of the precursors, activating medium and curing conditions influence the strength development and environmental impact of the geopolymer binder (Yazdi et al. 2018). In a previous study, fly ash/metakaolin-based geopolymer bonded products were produced for outdoor applications (Olayiwola et al. 2021). The mineral characteristics of the precursor materials required a high alkali concentration and elevated curing temperature to develop adequate strength properties. Products produced with 12 M NaOH and an elevated curing temperature of 100 °C had comparable properties to cement-bonded particleboards for outdoor applications. However, the economic and environmental implications associated with high alkali dose, coupled with the energy consumption to obtain the necessary temperature could have a detrimental effect on the acceptance of geopolymer products as ‘truly’ green alternatives to cement products. From an environmental aspect, geopolymer composites, which require a lower alkali dose and are curable in ambient conditions are desirable. Many investigations have considered substituting fly ash with ground granulated blast slag (GGBS) in a bid to eliminate elevated temperatures for curing and reduce the alkali dosage requirement. The compressive strength of the composite products obtained ranged from 36 to 100 MPa, while the flexural strength ranged from 7 to 10 MPa (Allahverdi et al. 2011; Guo and Pan 2018; Yazdi et al. 2018).

This study, aimed at finding beneficial use for the huge amounts of forest waste from the clearing of alien wood species and industrial residues such as slag being generated in South Africa, is a follow-up investigation to the previous study by Olayiwola et al. (2021). Biomaterial residues, ash and slag constitute about 74 million tons of waste landfilled in South Africa yearly (DEA 2012). These waste streams represent a valuable source of raw materials to produce geopolymer bonded products, which could find use in the provision of sustainable building components. The products were tested to technical specifications for cement-bonded particleboards according to EN 634–2 (2007).

2 Materials

2.1 Lignocellulosic materials and slag

Acacia wood samples (*A. saligna* and *A. mearnsii*) were provided by Casidra (SOC) Ltd, Paarl in the Western Cape, South Africa, while bagasse fibres were supplied by TBS Sugars Pty Ltd, South Africa. Wood preparation entailed debarking, chipping, and milling in a hammer mill fitted with a 1 mm sieve. Samples were stored in a conditioning

room at 20 °C and 65% relative humidity (RH) for 96 h before use. The slag used was a ground granulated blast slag with a specific gravity of 1.54, supplied by Afrimax, Cape Town, South Africa.

2.2 Chemical activator

Sodium silicate (SS), branded as Silchem 2008, with a silica modulus of 2, was supplied by PQ Silicas, South Africa. Analytical grade sodium hydroxide (SH) pellets of 98% purity were purchased from Merck Chemical (Pty) Ltd, SA. The two chemicals were mixed at a fixed weight ratio of SS:SH = 2.5:1 to form the chemical activator.

3 Methods

3.1 Material characterization

Determination of the chemical composition of the lignocellulosic materials was carried out according to the National Renewable Energy Laboratory Analytical Procedure (NREL LAP 013). The ash content was calculated using TAPPI Standard (T211 2012), while the bulk density was determined as a ratio of the mass of oven-dry samples placed in a 25 ml cylinder to the volume of the cylinder (Miranda et al. 2012). The particle size distribution (PSD) of the slag material was analysed using Saturn Digitizer 5200 V 1.12 operated at an ultrasonic intensity and flow rate of 60% and 12.0 l/min, respectively. The chemical composition of the slag was determined with an X-ray fluorescence (XRF) spectrometer. Fourier transform infrared spectroscopy (FTIR) was used to qualify the nature of molecular bonds existing in the LMs and the slag. The FTIR was performed using Thermo Scientific Nicolet iS10 Spectrometer equipped with a Smart iTR attenuated total reflectance (ATR) accessory. X-ray diffraction (XRD) of the slag was carried out using a Bruker D2 Phaser diffractometer with $\text{CuK}\alpha$ ($\lambda = 1.5418 \text{ \AA}$) at 3 kV and 10 mA. The diffraction intensities were captured with a Lynxeye detector with 2θ scans in the range 4–50° with a 0.020° step size. Images of the samples were captured using a Zeiss EVO® MA15 scanning electron microscope (SEM) in backscattered electron (BSE) mode for microstructural analysis.

3.2 Chemical activation

A solution of sodium hydroxide was prepared a day before use since the dissolution of pellets in water is an exothermic reaction, evolving a great amount of heat. The ratio of slag to the chemical activator was kept constant at 2:1. The molar concentration of sodium hydroxide was varied between 4 and 8 M according to the experimental design (Table 1).

Table 1 Details of the experimental design

Runs	Slag (g)	LM (g)	Na ₂ SiO ₃ (g)	NaOH (g)	MConc	Curing (°C, h)
1	160	40	57.14	22.86	4	25, 24
2	160	40	57.14	22.86	6	25, 24
3	160	40	57.14	22.86	8	25, 24
4	160	40	57.14	22.86	4	40, 6
5	160	40	57.14	22.86	6	40, 6
6	160	40	57.14	22.86	8	40, 6
Control	190	–	67.86	27.14	6	25, 24

3.3 Experimental design

The major factors considered in the experimental design included curing temperature (CT), molar concentration of sodium hydroxide (MCon) and the type of lignocellulose material (LM). A mixed factorial design was established using MCon and type of LM at 3 levels and CT at 2 levels, with three replicates each. The LM content was kept constant at 25% of slag content. The design was laid out using the Statistica software version 13.3, and the details are shown in Table 1. Untreated LM was mixed with slag in a dry state for 3 min before a pre-determined amount of chemical activator was introduced and thoroughly mixed for 5 min. The control samples were made with 6 M NaOH and cured at 40 °C for 24 h. The mixture was moulded in a rectangular frame and cold-pressed at 100 psi for 5 min to obtain a final board dimension of 218 × 75 × 13 mm³.

Demoulded boards were left at ambient conditions for 1 h and then wrapped with aluminium foil to prevent moisture loss during curing. Due to the high calcium content of slag, relatively lower curing temperatures from room to 40 °C have been reported to be sufficient to initiate setting and strength development (Li et al. 2018; Rashad 2015; Shi et al. 2018). In this study, the boards were cured at ambient conditions (25 ± 2 °C) and at 40 °C for 24 h. Thereafter, the boards were placed in a temperature and humidity-controlled environment for 27 days prior to testing.

3.4 Physical and mechanical tests

The physical and mechanical properties of the boards were tested following the ASTM D1037 standards (ASTM 2013). The physical tests included apparent density, water absorption, thickness, and volumetric swelling. A 3-point bending test was conducted with an Instron machine fitted with a 5 kN load cell and operated at 5 mm/min to evaluate the modulus of rupture (MOR) and apparent modulus of elasticity (MOE) of the boards. The dimensions of the test samples for mechanical and sorption tests were 218 × 75 × 13 mm³ and 75 × 50 × 13 mm³, respectively. The thermal stability of the boards was investigated using thermogravimetric analysis (TGA). The test was performed under nitrogen gas purge, at a flow rate of 40.0 ml/min and a ramp rate of 10 °C/min to 600 °C using a TA Instruments model Q500.

4 Results and discussions

4.1 Chemical composition and bulk density of lignocellulosic materials

The chemical composition of the different lignocellulosic materials (LMs) is presented in Table 2. The compositions of the Acacia species (*A. saligna* and *A. mearnsii*) are quite different from the sugarcane bagasse (SCB). SCB

Table 2 Chemical composition of the lignocellulosic materials

Parameters (%)	Lignocellulosic materials		
	<i>A. saligna</i>	<i>A. mearnsii</i>	SCB
Lignin	24.41 (2.52)	23.85 (1.25)	26.84 (2.18)
Hemicellulose	19.05 (0.86)	20.29 (0.11)	10.75 (1.01)
Cellulose	31.54 (0.48)	33.72 (0.13)	23.78 (0.46)
Water Extractives	5.51 (0.17)	5.52 (0.75)	9.72 (0.10)
EtOH Extractives	0.54 (0.04)	0.61 (0.09)	1.72 (0.02)
Total Extractives	6.08 (0.11)	6.37 (0.58)	11.49 (0.07)
Ash	0.67 (0.02)	0.71 (0.03)	3.99 (0.62)
Moisture content	6.94 (0.09)	7.43 (0.01)	5.90 (0.04)
Bulk density (kg/m ³)	181.43 (5.48)	162.38 (2.59)	119.66 (3.48)

Values in parentheses are the standard deviations

Table 3 Size distribution of slag material

Parameter	d ₁₀	d ₅₀	d ₉₀
Particle size (μm)	2.361	16.554	52.742

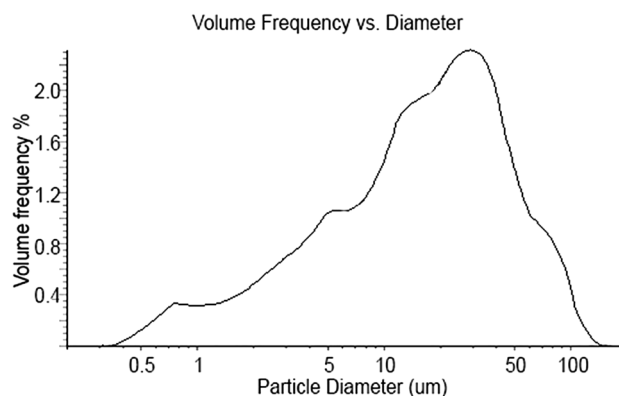
had a higher extractives, ash, and lignin content than the two Acacia species. Similar observations were reported by Amiandamhen et al. (2018a). The Acacia species also had higher holocellulose content and bulk density, which could be responsible for their superior board properties compared to SCB boards.

4.2 Characterization of slag material

The particle size distribution of the slag is presented in Table 3. The slag had fine particle sizes, with 50% less than 16.554 μm. Figure 1 shows that most of the particles are in the size range of 10–40 μm. This conforms with the particle size requirements proposed by Fernandez-Jimenez et al. (2008) for geopolymer precursors. Table 4 shows the chemical composition of the slag. The main components were SiO₂ (38.90%), CaO (33.92%), and Al₂O₃ (15.76%).

4.3 Physical properties of the boards

The physical and mechanical properties of the geopolymer boards are shown in Table 5. The boards had densities between 1 and 1.5 g/cm³ and were hence classified as high-density boards according to the American National Standard for composite panels ANSI-A208.1 (1999). The unit weights of the boards ranged from 11.59 to 14.53 kN/m³, 11.78 to 14.33 kN/m³, and 12.47 to 14.44 kN/m³ for *A. mearnsii* (AM), *A. saligna* (AS), and SCB boards, respectively. These

**Fig. 1** Particle size distribution of slag

values are lower than those typically reported for geopolymers in the literature (Andini et al. 2008; Chen et al. 2014; Cioffi et al. 2003). The values are in the range reported in a similar study by Olayiwola et al. (2021) using acacia and SCB particles in geopolymer matrix formulated with a combination of fly ash and metakaolin.

The sorption properties, indicated by water absorption (WA), thickness and volumetric swelling (TS/VS), were evaluated by immersing the boards in fresh water for 24 h. The test was carried out in a closed steel water bath maintained at 20 °C. The acacia boards had WA of 13.69–14.46% for AM and 7.16–17.28% for AS. The WA of SCB boards ranged from 17.69 to 21.48%. The TS and VS for AM boards ranged from 0.12 to 0.27% and 0.18–0.51%, respectively. The TS and VS were higher for AS and SCB boards. The ranges were 0.14–0.72% and 0.22–1.87% for AS; and 0.74–2.60% and 0.98–3.45% for SCB boards, respectively. All the boards met the sorption requirements for particle-boards according to the British Standard (EN634-2 2007).

Table 4 Chemical composition of slag (%)

Al ₂ O ₃	CaO	Cr ₂ O ₃	Fe ₂ O ₃	K ₂ O	MgO	MnO	Na ₂ O	P ₂ O ₅	SiO ₂	TiO ₂	L.O.I
15.76	33.92	–	0.15	1.01	8.64	0.87	0.24	0.01	38.90	0.72	–1.15

Table 5 Physical and mechanical properties of the boards

Boards	Board properties						
	MOE (MPa)	MOR (MPa)	Density (gcm ⁻³)	Unit weight (KNm ⁻³)	WA (%)	TS (%)	VS (%)
<i>A. mearnsii</i>	1720–5078	5.79–7.17	1.18–1.48	11.59–14.53	13.69–14.46	0.12–0.27	0.18–0.51
<i>A. saligna</i>	3410–7212	6.75–9.40	1.20–1.46	11.78–14.33	7.16–17.28	0.14–0.72	0.22–.87
SCB	1175–2934	5.24–7.90	1.27–1.47	12.47–14.44	17.69–21.48	0.74–2.60	0.98–3.45
Control	3895(174)	5.17(0.03)	1.56(0.012)	15.29(0.12)	10.66(0.372)	0.09(0.003)	0.13(0.020)
Standard*	≥4000**	≥9.0	≥1.0	-	≤25	≤15	≤15

*EN 634-2:2007; **Class 1 ≥4500, Class 2=4000; values in parentheses are standard deviations

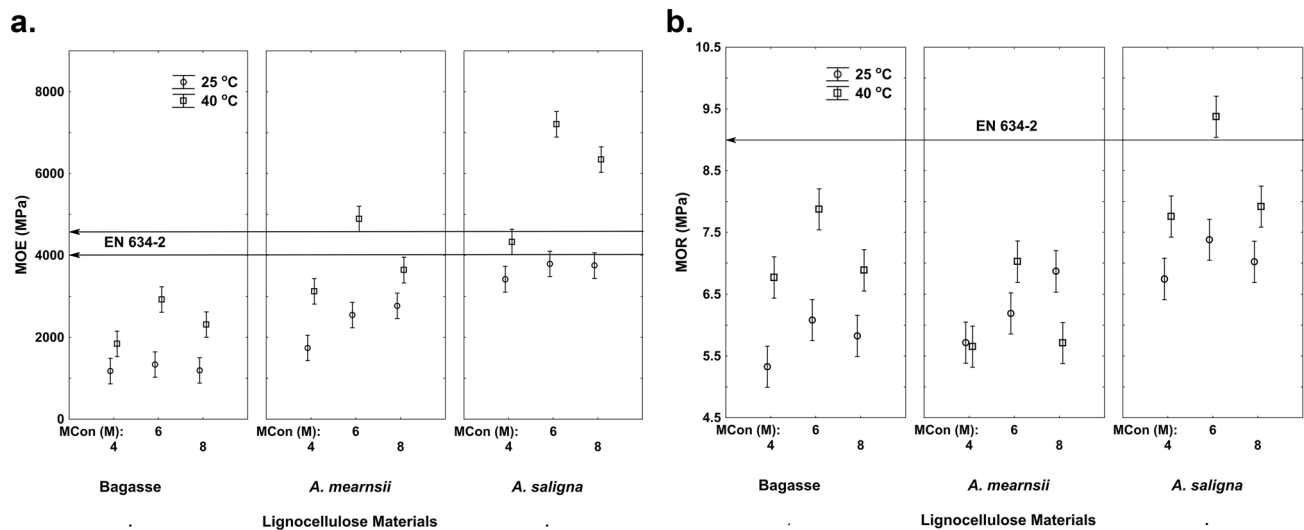


Fig. 2 Mechanical properties of all boards **a** MOE, **b** MOR (Vertical lines denote the confidence interval at 0.95)

4.4 Mechanical properties of the boards

Table 5 shows the mechanical properties of the boards. The static MOE and bending MOR are important requirements for inorganic bonded wood composite outdoor applications (EN634-2, 2007). The MOE of AM, AS and SCB boards ranged from 1720 to 5078 MPa, 3410–7212 MPa and 1175–2934 MPa, respectively. The MOR ranged from 5.79 to 7.17 MPa, 6.75–9.40 MPa and 5.24–7.90 MPa for AM, AS and SCB boards, respectively. According to the British standard (EN634-2, 2007), the minimum MOE and MOR of high-density particleboards are 4000 MPa and 9.0 MPa respectively, which indicates that only AS boards satisfied these requirements (Fig. 2). The strength properties of AM and SCB boards were not adequate based on EN 634 requirements, but they compared well with the requirements for low-density grade 1 & 2 particleboards, bonded with synthetic resin (ANSI-A208.1 1999). Hence, AM and SCB boards may be suitable for non-load bearing applications.

4.5 Influence of production variables on board properties

4.5.1 Effect of lignocellulosic material on board density and sorption properties

Lignocellulose materials have been reported to affect the properties of plastic and mineral bonded composites differently (Amiandamhen et al. 2016, 2018b; Na et al. 2014; Turku et al. 2016). The influence of LM on the board density is shown in Fig. 3(a). Boards made with AS had the highest mean density, which could be attributed to the

higher bulk density of AS which lowers the volume of incorporated particles. This ensured full encapsulation of the particles and lowered the ‘spring-back’ effect at high LM loading. According to Simatupang and Geimer (1990) and Amiandamhen et al. (2018b), improved properties of mineral-bonded composites require full encapsulation of wood/fibres in the matrix. Statistical analysis revealed that LM had a significant effect on the board density ($p < 0.05$) (Amiandamhen et al. 2018b). Although AM had a higher bulk density than SCB (see Table 2), there was no significant difference ($p > 0.05$) between the density of their respective boards. Olayiwola et al. (2021) reported that AM contained components that lower the geopolymerization reaction of fly ash/ metakaolin based geopolymer. Slag based geopolymer contains C – S – H, which is the main product of cement hydration (Song et al. 2000). Some wood species contain chemicals that inhibit the formation of C – S – H (Quiroga et al. 2016). Thus, the inhibitory components of AM could have delayed the formation of geopolymer products, leading to compromised microstructures.

Figure 3(b) shows how LM affects the sorption properties of the boards. SCB boards were the least dimensionally stable with the highest WA, TS and VS. SCB had a low bulk density and hence more volume per mass unit was required to produce the boards. It was observed that some SCB boards experienced problems of incompressibility, which resulted in the spring back effect after removal from the press. This caused the boards to expand and hence lowered their densities. High density indicates sufficient interlocking between the fibre and the matrix, forming a less porous microstructure (Amiandamhen et al. 2018a). The high density of AS explains why these boards had the best properties. Statistical

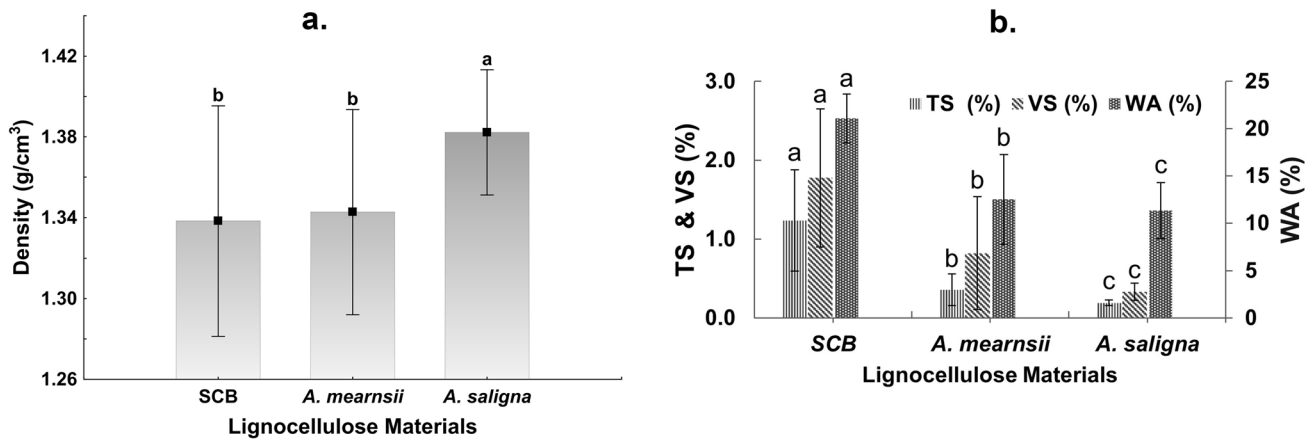


Fig. 3 Effects of LM on **a** density and **b** sorption properties. (Vertical lines denote standard deviations, series with same letters are not significantly different)

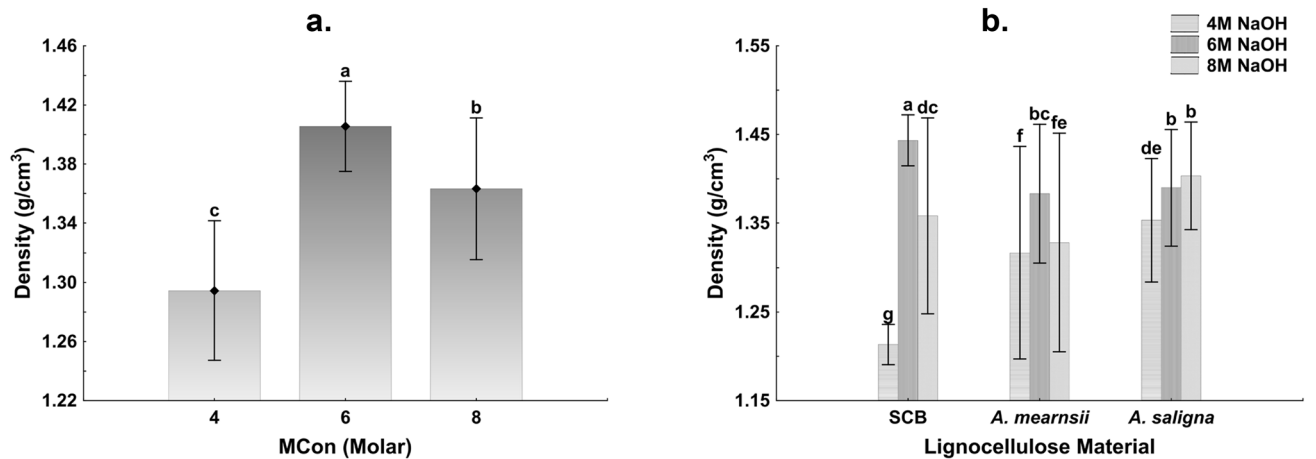


Fig. 4 Effect of molar concentration on **a** density of all boards, **b** density of each LM board. (Vertical lines denote standard deviations, series with same letters are not significantly different)

analyses revealed that WA, TS, and VS are significantly different for each LM ($p < 0.05$).

4.5.2 The effects of molar concentration on board density and sorption properties

The concentration of the activating medium is an important factor, which influences the strength development of geopolymer products (Petermann and Saeed 2012). The effect of molar concentration of the activator (MCon) on board density is presented in Fig. 4(a). The mean board density increased by 7.6% when the MCon was increased from 4 to 6 M. The increase was due to higher alkali dosage, which was sufficient to enhance the dissolution stage of geopolymer reaction. A similar observation was reported by Olayiwola et al. (2021) using fly ash/ metakaolin-based geopolymer. A reduction in mean board density by about 2.86%

was observed when the MCon was further increased to 8 M. The reduction is attributed to excess alkali ions, which deteriorated the microstructure of the composite. As seen in Fig. 4(b), this observation was consistent for SCB and AM boards only, because the density of AS boards slightly increased when the MCon was increased to 8 M. However, there was no significant difference in MCon between 6 and 8 M for AS boards.

Figure 5 shows the influence of MCon on the WA, TS, and VS of the boards. The dimensional stability of the boards followed a similar trend to the density. The TS/VS decreased when the MCon increased to 6 M and then increased when MCon was increased to 8 M. This indicates that the microstructure of the 8 M boards was porous and aided water uptake. The mineralized wood particles at higher alkali dosage (8 M NaOH) left large pores, which provided additional channels and exposed more sorption

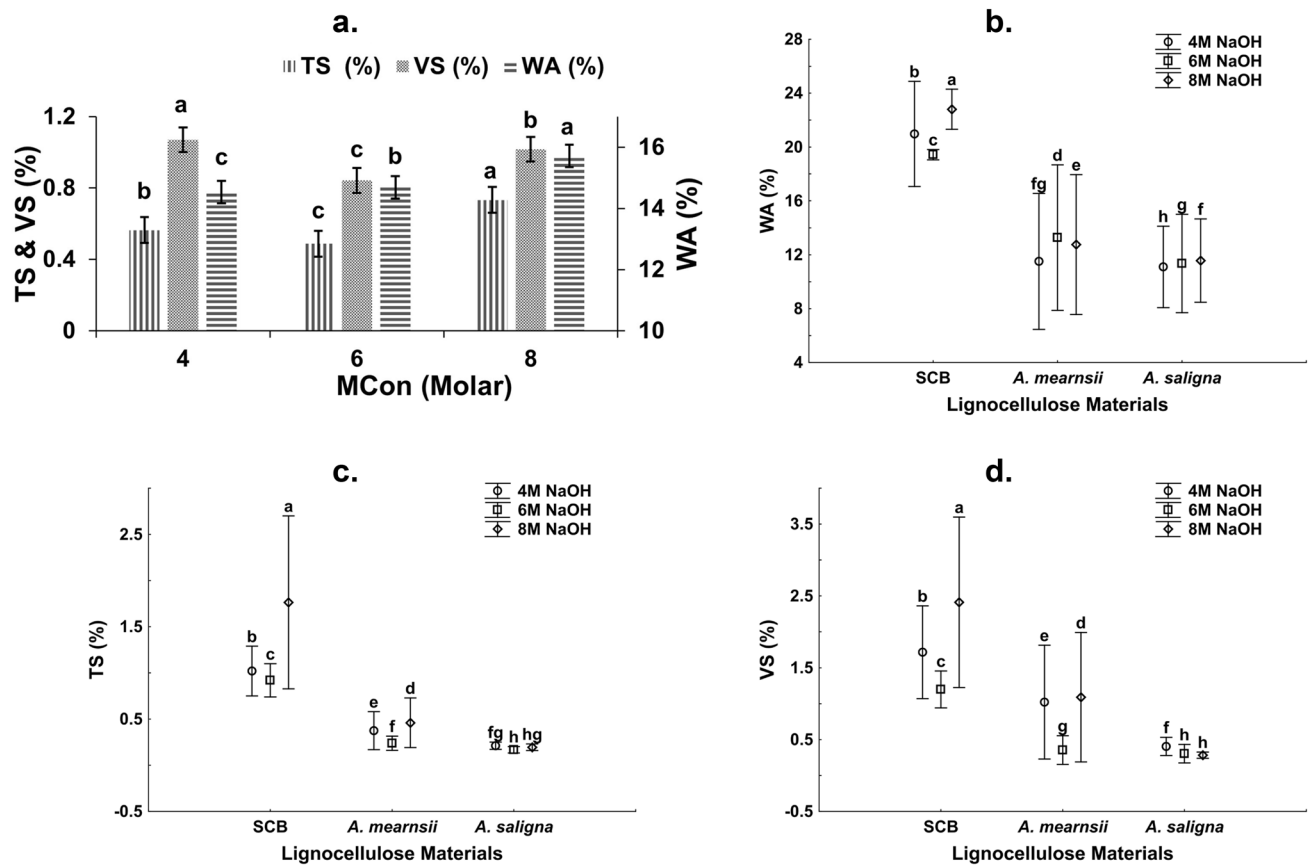


Fig. 5 Effects of MCon on sorption properties: **a** WA, TS, and VS of all boards, **b** WA of each LM board, **c** TS of each LM board, **d** VS of each LM board. (Vertical lines denote standard deviations, series with same letters are not significantly different)

sites for water molecules. The boards produced with 8 M absorbed more water and were the least dimensionally stable. A variation however existed in the trend due to differences in the chemical composition of the LM.

Figure 5(b) shows the mean WA for each LM. The mean WA for AM boards produced with 6 M was higher than those made with 4 M and 8 M, but their mean TS/VS were lower. The higher WA of AM boards could be due to the high cellulose and hemicellulose contents of AM, which provided numerous sorption sites for water molecules. However, 6 M produced boards with sufficiently compact structure to resist the impact of water uptake. A slight, but significant difference in WA was observed in AS boards at all MCon levels ($p < 0.05$). 8 M boards had slightly higher mean WA and TS than 6 M boards, but the VS was lower. Figure 5 (c & d) shows that there was no significant difference ($p > 0.05$) between the mean TS and VS for AS boards made with 6 M and 8 M MCon.

4.5.3 The effects of curing temperature on density and sorption properties

Increasing the curing temperature enhances the reactivity and rate of dissolution of the precursor materials (Petermann and Saeed 2012). Figure 6(a) shows that the curing temperature had a significant effect on the board density ($p < 0.05$). The mean density of the boards increased by about 8.5% when the temperature was increased to 40 °C. However, the board density of a binary fly ash/metakaolin (FK/MK) geopolymer was reduced when the curing temperature was increased to 100 °C (Olayiwola et al. 2021). The elevated temperature induced rapid moisture removal causing the formation of numerous micropores. Figure 6(b) shows that boards cured at 40 °C absorbed more water but were more dimensionally stable than those cured at room temperature. The WA increased by about 44%, while the

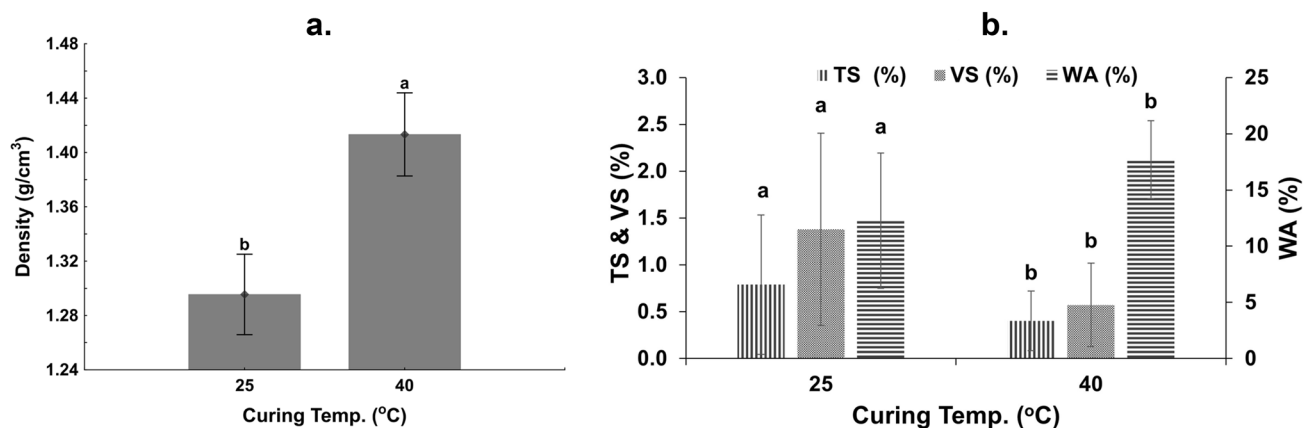


Fig. 6 Effects of curing temperature on physical properties: **a** board density and **b** sorption. (Vertical lines denote standard deviations, series with same letters are not significantly different)

TS and VS decreased by 49% and 58%, respectively. The higher temperature improved dissolution of Ca^{2+} , Al^{3+} and Si^{2+} species and enhanced the polycondensation process to form a compact product (see Sect. 4.7.3). Water, which is a by-product of the condensation stage formed and dried quicker at 40 °C than at 25 °C. This created more micropores which provided more channels for water uptake. A similar phenomenon was reported by Tran et al. (2009). Reduction in TS and VS showed that the fibre-matrix bond was not strong enough to resist dimensional changes associated with an increase in WA.

Figure 7 shows how the curing temperature affected the density and sorption properties of each LM. The density and WA of each LM increased as the temperature increased, while the TS and VS decreased. There was a significant difference in the mean density, WA, TS and VS between the curing temperatures for each LM ($p < 0.05$).

4.6 Influence of production variables on the mechanical properties

Figure 8 shows that all the production variables had significant effects on the mechanical properties of the boards. The MCon had significant interactions with LM and curing temperature on the MOE, as displayed in Fig. 8(a). Figure 8(b) shows that only the interaction between LM and MCon had a significant effect on the MOR, while the other interactions had no significant effects.

4.6.1 Effects of MCon on strength properties

The rate of hydration of slag depends on its composition and the concentration of the alkali activator (Song et al. 2000). Figure 9 shows how MCon affects the mechanical properties of all boards. Figure 9 (a & b) indicates that a significant

difference existed between the alkali concentrations, with 6 M having the highest mean MOE and MOR. The MOE and MOR increased by about 46% and 16% respectively, when the MCon was increased to 6 M. Bilim et al. (2013) also reported an increase in the compressive strength of alkali-activated slag with an increase in NaOH concentration. Sufficient dissolution of the anions in the slag by the cations in the alkaline activator improved the microstructural development of the product, leading to enhanced mechanical properties. However, MOE and MOR were reduced when MCon was further increased to 8 M. This is attributed to the excess alkali ions, which mineralized the wood particles, leading to a reduction in the stress-bearing capacity of the particles in the matrix. Efflorescence was observed on the boards, and the SEM image in Fig. 10 shows the formation of bicarbonate indicating excessive alkali ions. Provis and van Deventer (2014) stated that efflorescence is not always harmful to the structural integrity of the products. However, in this case, it is evident that the excess alkali ions compromised the microstructure of the composites. Figure 9(c & d) indicates that the trend was consistent for the MOE and MOR of each LM. Boards produced with 4 M MCon had the lowest MOE and MOR, although there was no significant difference in the MOE of SCB and the MOR of SCB and AS boards made with 4 M and 8 M MCon. Although MCon of 6 M had a higher mean MOR, there was no significant difference between those of 6 M and 8 M for AM boards. The variation is due to difference in their chemical composition.

4.6.2 Effects of curing temperature on strength properties

Curing temperature has a significant influence on the strength development of activated slag materials. Figure 11 shows that there is a significant difference between the curing temperature on both MOE and MOR of all boards.

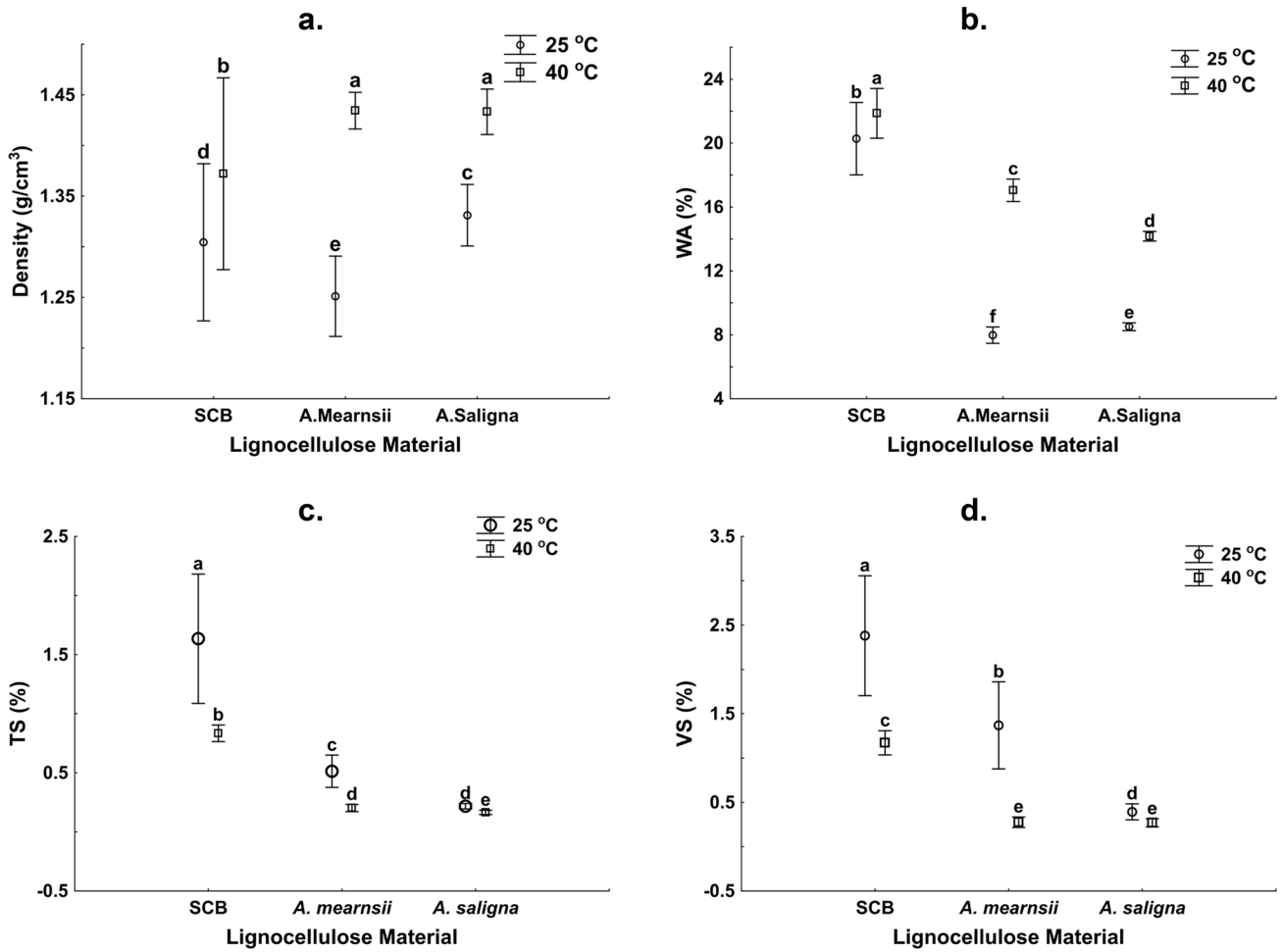


Fig. 7 Effects of curing temperature on **a** density, **b** WA, **c** TS and **d** VS of each LM board. (Vertical lines denote standard deviations, series with same letters are not significantly different)

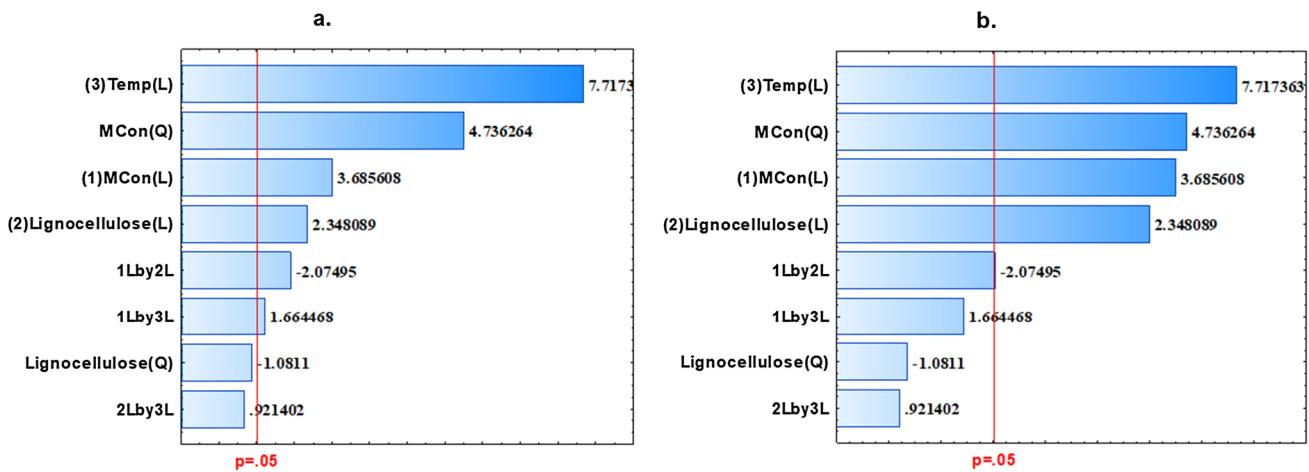


Fig. 8 Pareto charts showing the effects of production variables and their interactions on (a) MOE and (b) MOR. (1-Mcon, 2-LM, 3- Curing temperature, L- Linear effect, Q-Quadratic effect. Bars that cross the p-line are significant)

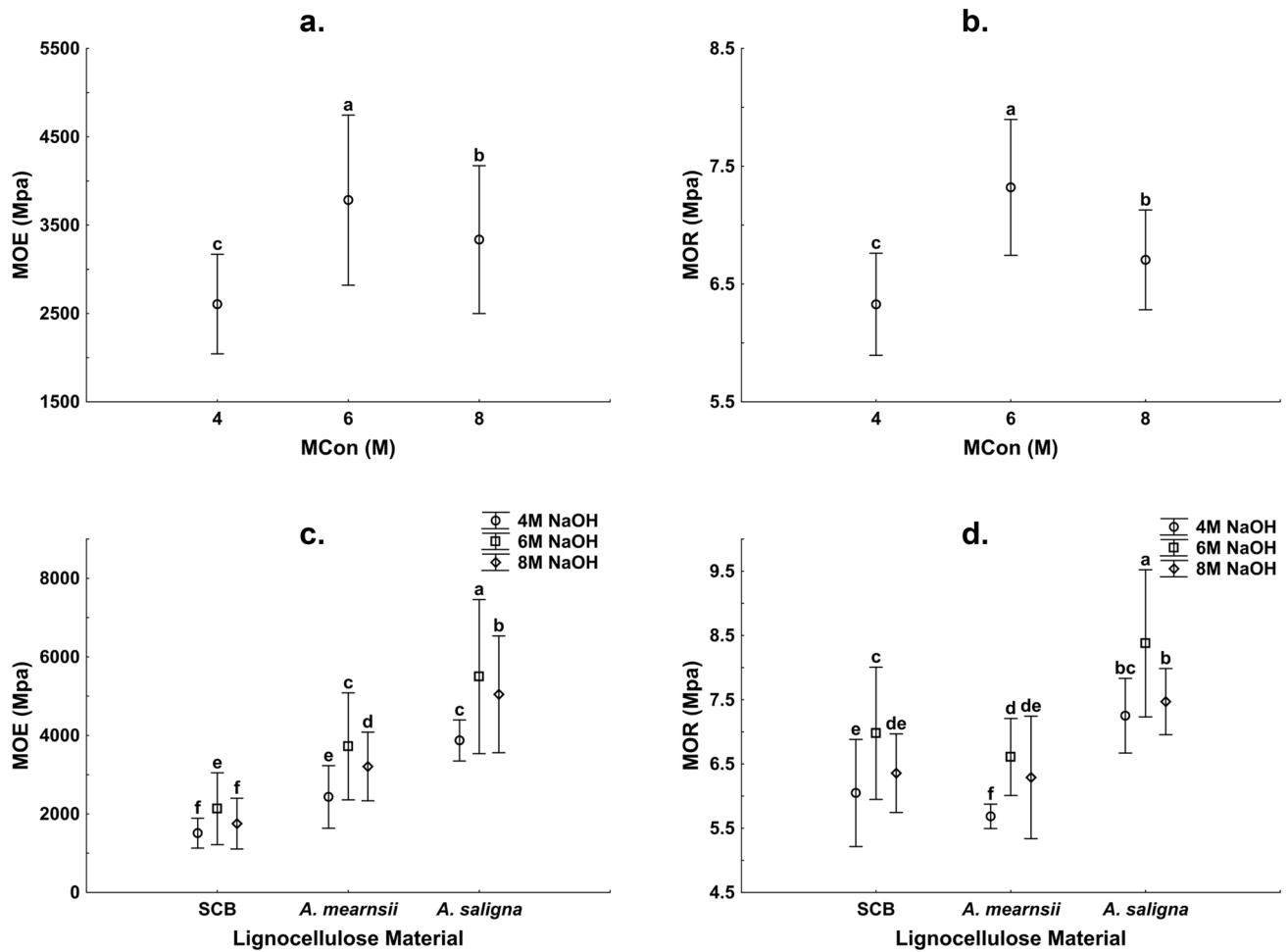


Fig. 9 Effects of **a** MCon on MOE, **b** MCon on MOR, **c** MCon and LM on MOE and **d** MCon and LM on MOR. (Vertical lines denote standard deviations, series with same letters are not significantly different)

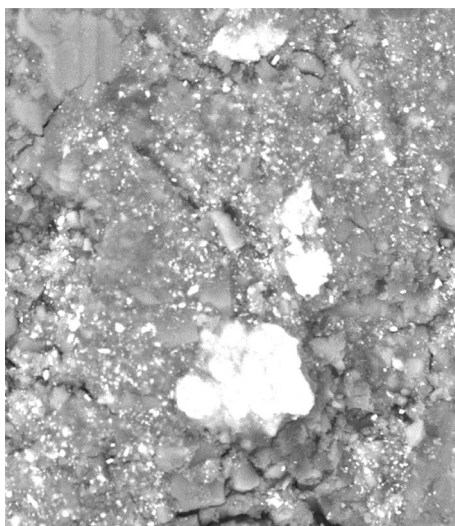


Fig. 10 Formation of bicarbonate in SCB board due to excessive alkali ions

Boards cured at 40 °C had higher mean MOE and MOR. The MOE and MOR increased by about 45% and 14%, respectively when the temperature was increased from 25 °C to 40 °C. Bilim et al. (2013) studied alkali-activated slag (AAS) mortars subjected to different curing conditions and reported that heat curing considerably accelerated the early strength development and reduced the high shrinkage of AAS mortar. However, the strength decreased at later age due to dry curing at 50% RH after heat treatment. The SCB and acacia boards were wrapped with aluminium foil before curing and left to cool down to 28 ± 2 °C in the oven. This prevented rapid water removal and excessive drying shrinkage, which has been reported to be the main cause of crack development and expansion. Apart from the MOR of AM boards, the mechanical properties of the boards improved at 40 °C. AM boards cured at 25 °C had a slightly higher mean MOR than those cured at 40 °C but the difference was not significant ($p > 0.05$). AS boards cured at 25 °C had higher

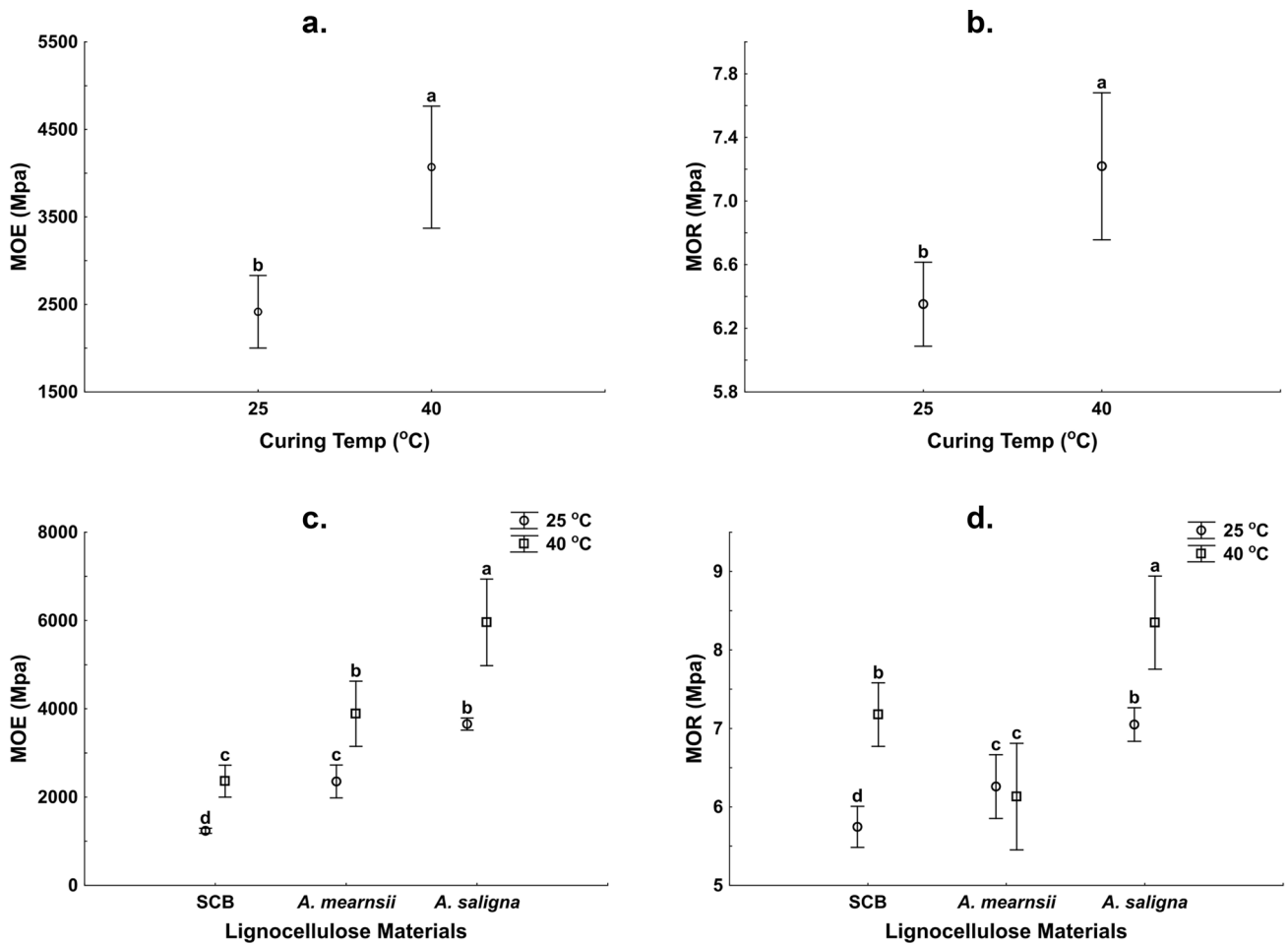


Fig. 11 Effects of **a** curing temperature on MOE, **b** curing temperature on MOR, **c** curing temperature and LM on MOE and **d** curing temperature and LM on MOR. (Vertical lines denote standard deviations, series with same letters are not significantly different)

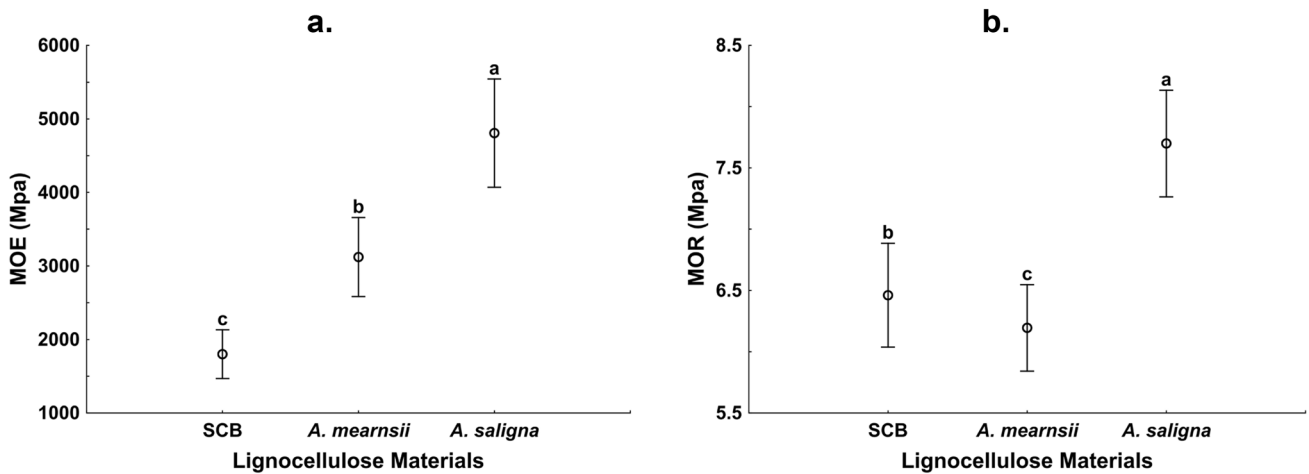


Fig. 12 Effects of LM on mechanical properties **a** MOE and **b** MOR. (Vertical lines denote standard deviations, series with same letters are not significantly different)

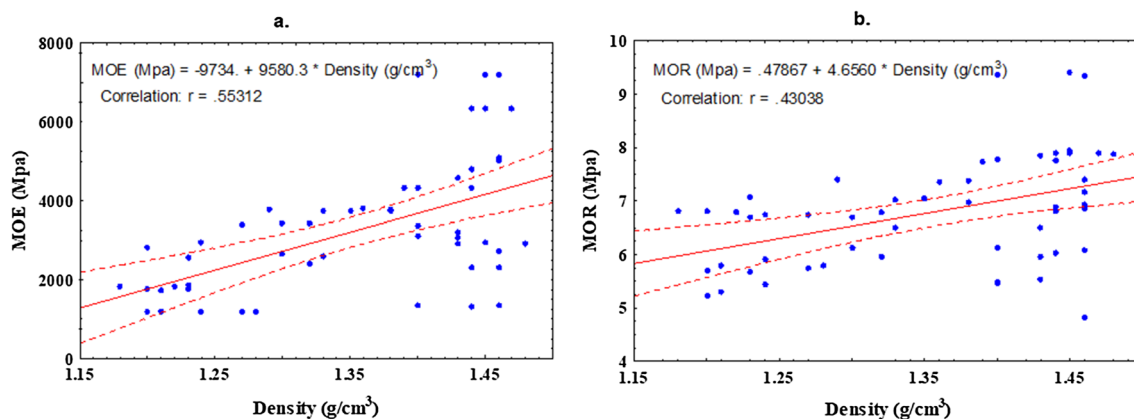


Fig. 13 Relationships between density and **a** MOE and **b** MOR

MOE than SCB boards cured at 40 °C and were not significantly different from AM boards cured at 40 °C.

4.6.3 Effect of LM on MOE and MOR

Figure 12 shows that there were significant differences in the strength properties between the LMs. The MOE and MOR followed a similar pattern to the density for acacia species. AS boards had the highest mean MOE and MOR, which can be ascribed to the higher cellulose and lignin contents of AS. Higher lignin and cellulose contents improve the strength of composite products by forming strong interfacial adhesion between the particles and the matrix (Bledzki et al. 1998; Bledzki and Gassan 1999). Figure 13 shows a positive correlation between board density and strength properties. The observation was in line with those of phosphate-bonded composites (Amiandamhen et al. 2018b) and fly ash/ metakaolin based geopolymers bonded composites (Olayiwola et al. 2021). However, there was a change in the trend between SCB and AM boards. Although AM boards had a slightly higher mean density than SCB (the difference was not significant), there were significant differences in their mean MOE and MOR. AM boards had a higher mean MOE but lower mean MOR than SCB boards. This could be due to the difference in their chemical compositions. AM contained higher hemicellulose and cellulose, but lower lignin than SCB. Interaction between these components and binding systems at the different stages of the geopolymerization process could affect the strength properties differently.

4.6.4 Effects of interaction between MCon and curing temperature on the strength properties

Figure 14 shows the influence of the interactions between MCon and the curing temperature on the MOE. Figure 14(a) shows that boards cured at 40 °C had higher mean MOE than those cured at 25 °C at all levels of MCon. Statistical

analyses also revealed that there was a significant difference between the curing temperature at each MCon level on the MOE ($p < 0.05$). Boards made with MCon of 6 M and cured at 40 °C had the highest MOE. However, there was no significant difference between MCon of 6 M and 8 M for boards cured at 25 °C ($p > 0.05$). Figure 14(b) shows the influence of MCon and curing temperature on each LM. For SCB and AS boards, there were no significant differences between MCon of 4 M, 6 M, and 8 M for boards cured at 25 °C. AM boards produced with MCon of 4 M and cured at 25 °C had the lowest mean MOE and were significantly different from those made with 6 M and 8 M MCon. Curing at 40 °C exhibited a similar trend for each LM. The highest mean MOE was recorded for each LM produced with 6 M MCon.

The influence of the interaction between MCon and curing temperature on MOR is shown in Fig. 15. Figure 15(a) shows that the mean MOR increased with the curing temperature at each MCon level. However, the analysis revealed that the curing temperature had no significant effect on the mean MOR at 8 M MCon. It was also observed that the mean MOR of boards made with 4 M MCon and cured at 40 °C was not significantly different from those produced with 8 M MCon. Figure 15(b) shows that the interactions between MCon and curing temperature affected the MOR of the boards for each LM differently. The mean MOR of SCB and AS boards increased as the curing temperature increased at each level of MCon. For AM boards, there was no significant difference in mean MOR at 4 M MCon and increasing the curing temperature significantly caused a reduction in the mean MOR at 8 M MCon.

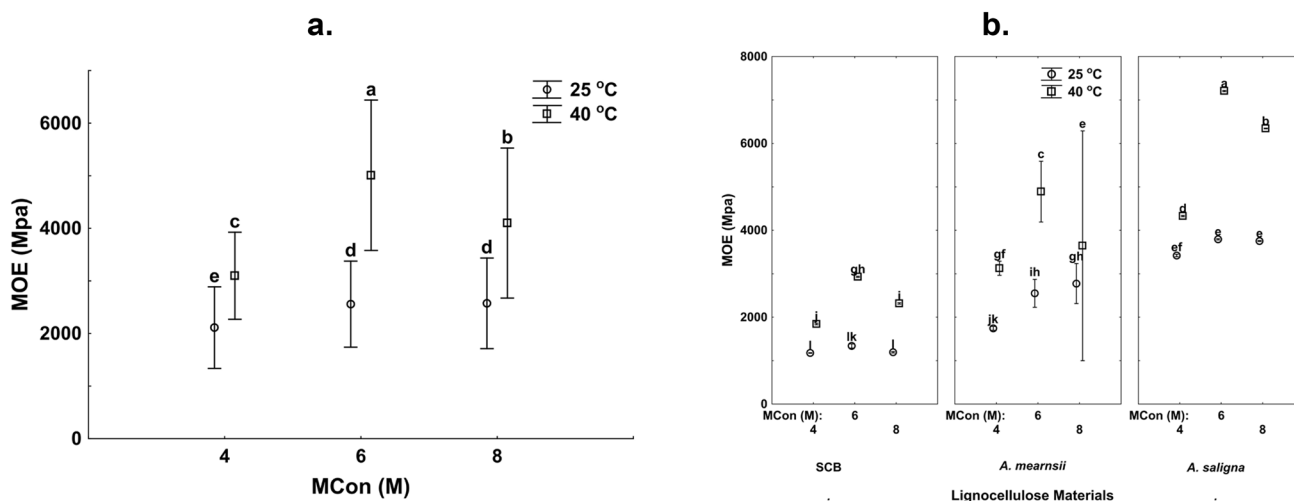


Fig. 14 Effects of MCon and temperature on MOE: **a** all boards and **b** each LM board. (Vertical lines denote standard deviations, series with same letters are not significantly different)

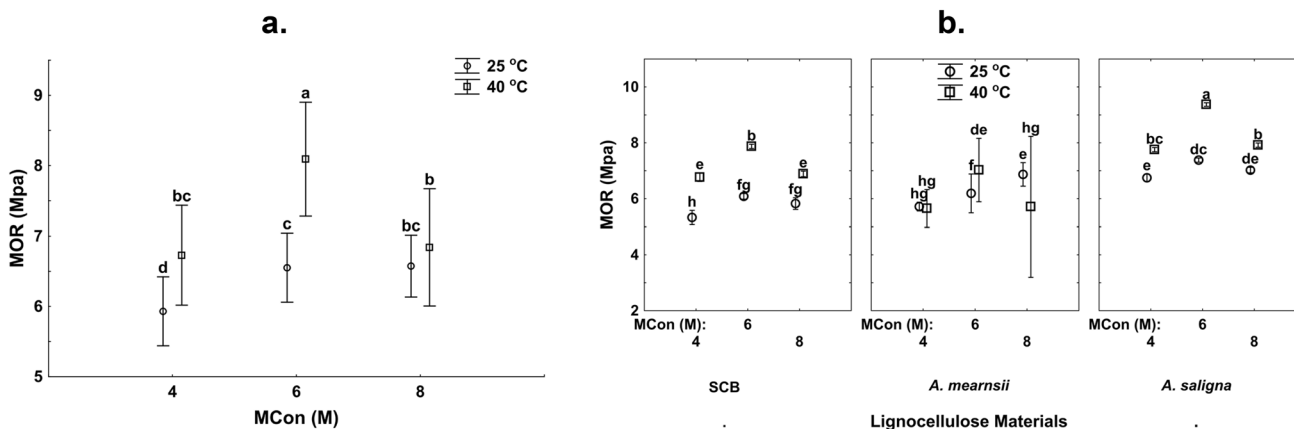


Fig. 15 Effects of MCon and curing temperature on MOR: **a** all boards and **b** each LM board. (Vertical lines denote standard deviations, series with same letters are not significantly different)

4.7 Material characterizations

4.7.1 Fourier transform infrared (FTIR) spectroscopy

Figure 16 shows the FTIR spectra of the LM boards. The peaks found around 1737 cm^{-1} and 2916 cm^{-1} in the spectra of the LM disappeared in the boards. The peak at 1737 cm^{-1} assigned to the carbonyl (C=O) stretching of acetyl groups of hemicellulose disappeared in the boards for all LM. Likewise, the peak around 2916 cm^{-1} attributed to the symmetric vibration of C–H and aliphatic axial decomposition in CH_2 and CH_3 groups from cellulose, lignin and hemicellulose was not found in the boards of any LM. The peaks in the band $1235 - 1254\text{ cm}^{-1}$, which was attributed to the C–O stretch of the acetyl group of lignin also disappeared. The

peaks at 1603 cm^{-1} and 1633 cm^{-1} assigned to the C–Ph vibration and C=C bonds of the aromatic lignin structure were present only in SCB. These peaks convoluted and shifted to 1636 cm^{-1} in the SCB boards. CH_2 symmetric bending of cellulose also shifted from 1422 cm^{-1} to around 1411 cm^{-1} and its intensity decreased in the boards. The shift in this peak and the absence of other peaks in the board indicate partial degradation of lower molecular components of the LM in the alkaline matrix. Similar observations were reported for FA/MK based geopolymer products. This confirms the assumption that the degraded components of the LM could have interfered with the geopolymer reactions and thus affect the properties of the composite products. The two prominent bands corresponding to the stretching vibrations of Al–O and Si–O in the precursor material (873 cm^{-1}

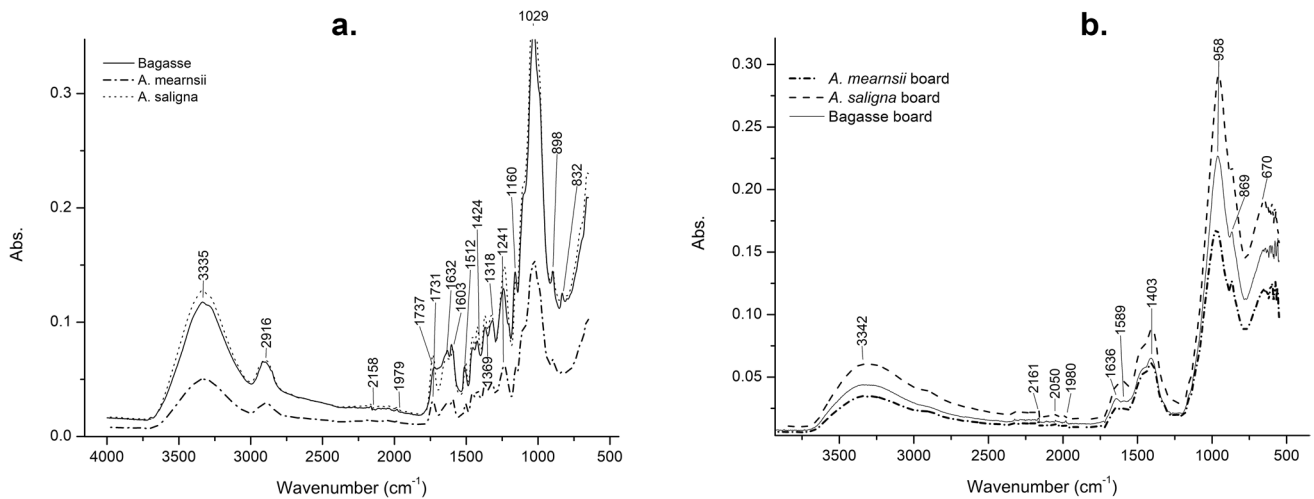


Fig. 16 FTIR spectra of **a** LM and **b** LM boards

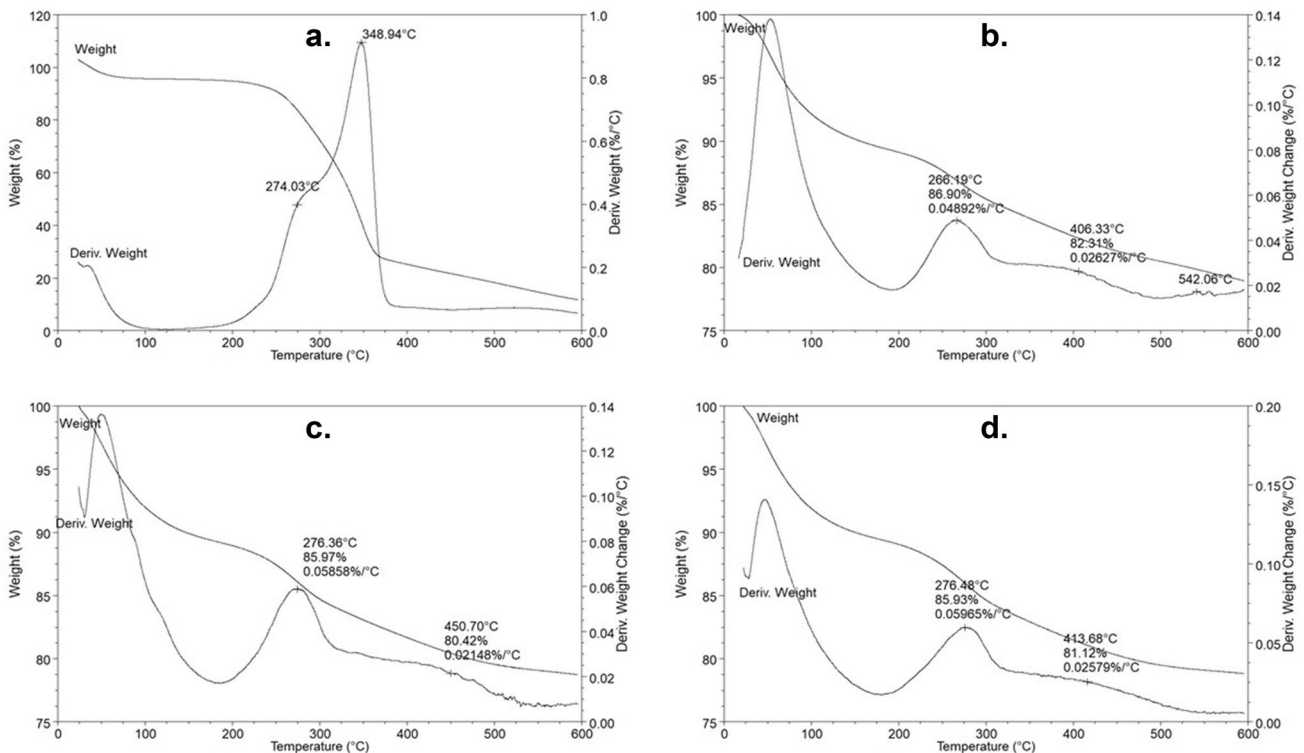


Fig. 17 Derivative and weight loss thermographs of **a** AS, **b** SCB boards, **c** AS boards and **d** AM boards

and 680 cm^{-1}) shifted towards the lower wavenumbers. This indicates partial replacement of silica species by alumina as a result of geopolymerization reactions (Criado et al. 2005; Davidovits 2008).

4.7.2 Thermogravimetric analysis (TGA)

TGA operated under nitrogen gas was employed to study the thermal stability of the LM and the geopolymer bonded composite products. Figure 17 shows the derivative thermographs (DTG) and weight loss of the boards and AS. The thermographs of SCB and AM have been reported in a

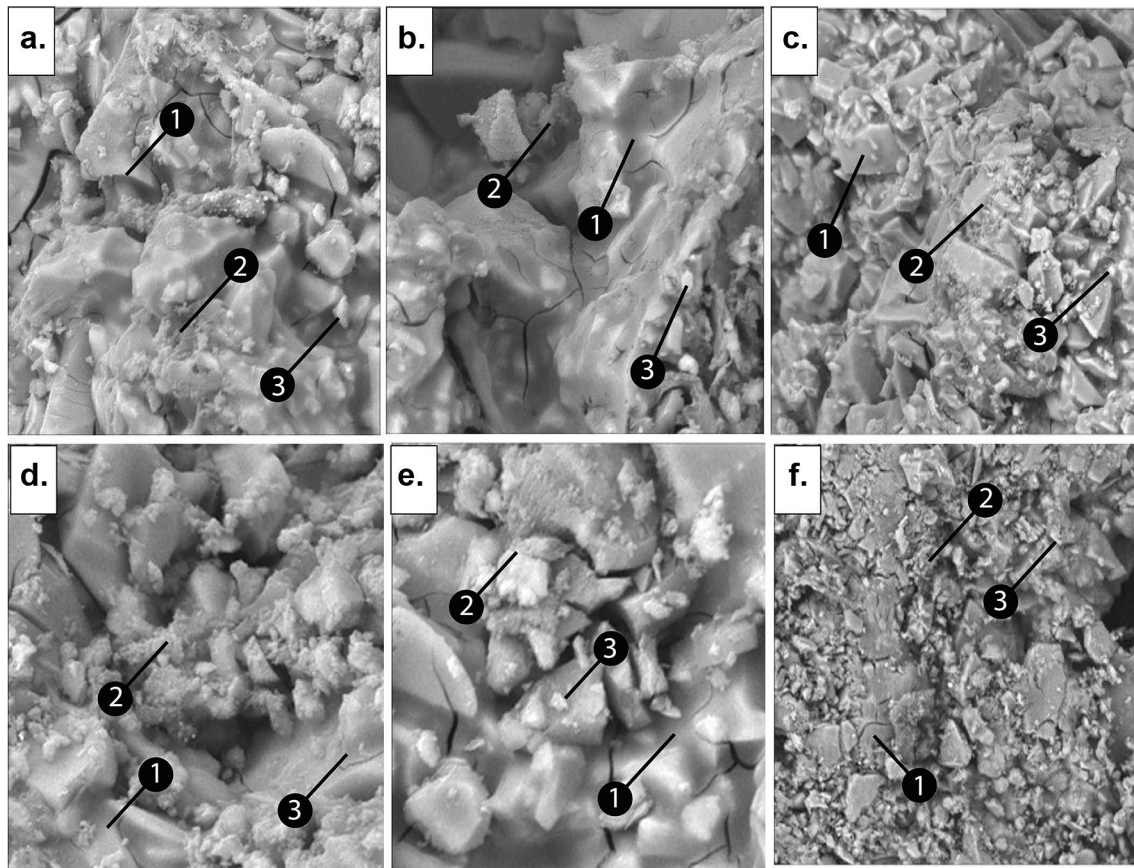


Fig. 18 SEM images of boards made with 6 M MCon and cured at 40 °C: **a** AS, **b** AM, **c** SCB boards cured at 25 °C, **d** AS, **e** AM and **f** SCB. 1-CASH, 2-CSH, 3-Unreacted particles

recent study (Olayiwola et al. 2021). The DTG peak below 200 °C is attributed to a loss of evaporable water. The main degradation peaks in the LM shifted to 276.36 °C, 266.19 °C and 276.48 °C for AS, SCB, and AM boards, respectively. These peaks were about 20 °C lower than the main degradation peaks in FA/MK geopolymer bonded boards (Olayiwola et al. 2021). The peaks fall within the lower end of cellulose degradation range of 275 °C – 500 °C (Machado et al. 2018). Like the FA/MK boards, the peak-shoulders found in the DTG of LM, which were attributed to the degradation of hemicellulose, are convoluted with cellulose, and lignin components were absent in the DTG of the boards.

These corroborate the FTIR results showing that lower molecular weight cellulose, lignin and hemicellulose components degraded in the alkaline matrix. Other broad peaks between 350 °C and 475 °C were noticeable in the boards. This could be attributed to the overlap of degradation of crystalline components of LM and the change of phases in the microstructure of the matrix at high temperatures. These peaks appeared later at about 100 °C in FA/MK geopolymer boards (Olayiwola et al. 2021). According to Pereira Ferraz et al. (2016), certain impurities, such

as inorganic salts could cause degradation of cellulose at lower temperatures. The disparity may be due to the difference in the components of the precursor materials and the geopolymerization products. A peak around 550 °C was present in SCB boards and another peak was building up shortly before the end of the thermal test. This could be attributed to the onset of thermal decomposition of the microstructure of the matrix. The rate of degradation of AM and AS boards was constant at this stage and no peak was further observed. The SCB boards contained higher volume per unit area due to their low bulk density. This could be responsible for the observed early decomposition of the microstructure. However, the products are thermally stable as the residues are all above 80%.

4.7.3 Scanning electron microscopy (SEM)

SEM was employed to study morphology and internal structure of the boards under different production conditions. Figure 18 shows the micrographs of boards produced with 6 M MCon. The images indicate the formation

of amorphous phases with a dense gel-like matrix. The boards have a uniform structure of condensed products believed to be calcium alumino-silicate hydrate (C – A – S – H) surrounded with microcrystals of calcium silicate hydrate (C – S – H). There are also numerous unreacted slag particles within the dense matrix. The unreacted particles could serve as fillers and improve the board properties. Boards cured at 40 °C had a more compact structure with fewer cracks than those cured at 25 °C. This could be due to increased reactivity and dissolution of Ca²⁺, Al³⁺ and Si⁴⁺ species at elevated temperature. These results support the physical and strength properties mentioned previously.

5 Conclusion

The study has demonstrated the feasibility of producing high-density slag-based geopolymer panels using South African alien invasive species and SCB. The proposed product could be used in exterior applications such as walls, flooring, and siding. The major findings are summarized as follows:

1. Curing temperature and MCon of the activator had significant effects on the properties of the slag-based geopolymer boards. Addition of lignocellulosic material improved the flexural properties of the products.
2. Curing at 40 °C influenced the reaction kinetics, enhanced microstructural properties and produced a dense geopolymeric matrix, which resulted in improved physical and mechanical properties. Boards cured at 25 °C had better strength than phosphate bonded wood composites reported in the literature.
3. Increasing MCon of the activator beyond 6 M caused the formation of bicarbonate and deteriorated the internal structure of AM and SCB boards due to excess alkali ions. 8 M MCon slightly increased the strength properties of AS boards, but the effect was not significantly different from 6 M MCon.
4. FTIR and TGA results confirmed the degradation of lower molecular lignocellulosic components in the alkaline matrix. Degraded products could lower geopolymeric reactions, but FTIR confirmed that geopolymerization took place. SEM images also revealed the formation of geopolymer and hydration products, which indicated that the degraded components did not prevent geopolymer setting.
5. All the boards met the sorption requirements for particleboards according to the British Standard. The strength properties of the boards were not adequate but they compared well with the requirements for low-density resin bonded particleboards grades 1 & 2 (ANSI-

A208.1). Hence, the boards may be suitable for non-load bearing applications in outdoor conditions.

6. The boards were thermally stable, as the residues retained at the end of thermal analysis were about 80%.

Funding This study was funded by the German Federal Ministry of Education and Research, Grant no: 01DG17007A, Martina Meincken, DAAD Project, Grant no: 57359374, Martina Meincken.

References

- Aiken TA, Sha W, Kwasny J, Soutsos MN (2017) Resistance of geopolymer and Portland cement based systems to silage effluent attack. *Cem Concr Res* 92:56–65. <https://doi.org/10.1016/j.cemconres.2016.11.015>
- Allahverdi A, Kani E, Yazdanipour M (2011) Effects of blast furnace slag on natural pozzolan- based geopolymer cement. *Ceramics-Silikáty* 55(1):68–78
- Alomayri T (2017) Effect of glass microfibre addition on the mechanical performances of fly ash-based geopolymer composites. *J Asian Ceram Soc* 5(3):334–340. <https://doi.org/10.1016/j.jasc.2017.06.007>
- Amiandamhen SO, Meincken M, Tyhoda L (2016) Magnesium based phosphate cement binder for composite panels: A response surface methodology for optimisation of processing variables in boards produced from agricultural and wood processing industrial residues. *Ind Crops Prod* 94:746–754. <https://doi.org/10.1016/j.indcrop.2016.09.051>
- Amiandamhen SO, Meincken M, Tyhoda L (2018a) The effect of chemical treatments of natural fibres on the properties of phosphate-bonded composite products. *Wood Sci Technol* 52(3):653–675. <https://doi.org/10.1007/s00226-018-0999-9>
- Amiandamhen SO, Montecuccoli Z, Meincken M, Barbu MC, Tyhoda L (2018b) Phosphate bonded wood composite products from invasive Acacia trees occurring on the Cape Coastal plains of South Africa. *Eur J Wood Prod* 76:437–488. <https://doi.org/10.1007/s00107-017-1191-x>
- Andini S, Cioffi R, Colangelo F, Grieco T, Montagnaro F, Santoro L (2008) Coal fly ash as raw material for the manufacture of geopolymer-based products. *Waste Manage*. <https://doi.org/10.1016/j.wasman.2007.02.001>
- ANSI-A208.1 (1999) Particleboards. American National Standard, Composite Panel Association
- ASTM (2013) ASTM D1037: Standard test methods for evaluating properties of wood-base fiber and particle. In *Annual Book of ASTM Standards* (issue July). <https://doi.org/10.1520/D1037-99>
- Bilim C, Karahan O, Atiş CD, Ilkentapar S (2013) Influence of admixtures on the properties of alkali-activated slag mortars subjected to different curing conditions. *Mater Des* 44:540–547. <https://doi.org/10.1016/j.matdes.2012.08.049>
- Bledzki AK, Gassan J (1999) Composites Reinforced with Cellulose Based Fibers. *Prog Polym Sci* 24:221–274
- Bledzki AK, Gassan J, Theis S (1998) Wood-filled Thermoplastic Composites. *Mech Compos Mater* 34(13):563–568
- Chen R, Ahmari S, Zhang L (2014) Utilization of sweet sorghum fiber to reinforce fly ash-based geopolymer. *J Mater Sci* 49(6):2548–2558. <https://doi.org/10.1007/s10853-013-7950-0>
- Cioffi R, Maffucci L, Santoro L (2003) Optimization of geopolymer synthesis by calcination and polycondensation of a kaolinitic

- residue. *Resour Conserv Recycl.* [https://doi.org/10.1016/S0921-3449\(03\)00023-5](https://doi.org/10.1016/S0921-3449(03)00023-5)
- Criado M, Palomo A, Fernández-Jiménez A (2005) Alkali activation of fly ashes. Part 1: Effect of curing conditions on the carbonation of the reaction products. *Fuel* 84(16):2048–2054. <https://doi.org/10.1016/j.fuel.2005.03.030>
- Davidovits J (2008) *Geopolymer Chemistry and Applications* (3rd ed.). Institute Geopolymere, Saint-Quentin, France
- DEA (2012) National Waste Information Baseline Report. Pretoria: Department of Environmental Affairs.
- EN634–2 (2007) Cement-bonded particleboards –Specifications-Part 2: Requirements for OPC bonded particleboards for use in dry, humid and external conditions. British Standards
- Fernandez-Jimenez A, Monzo M, Vicent M, Barba A, Palomo A (2008) Alkaline Activation of Metakaolin-Fly Ash Mixtures: Obtain of Zeoceramics and Zeocements. *Microp Mesop Mater* 108:41–49
- Guo X, Pan X (2018) Mechanical properties and mechanisms of fiber reinforced fly ash–steel slag based geopolymer mortar. *Constr Build Mater* 179:633–641. <https://doi.org/10.1016/j.conbuildmat.2018.05.198>
- Komnitsas KA (2011) Potential of geopolymer technology towards green buildings and sustainable cities. *Procedia Eng* 21:1023–1032. <https://doi.org/10.1016/j.proeng.2011.11.2108>
- Korniejenko K, Mikula J, Lach M (2015) Fly ash based fiber-reinforced geopolymer composites as the environmental friendly alternative to cementitious materials. *Proceed 2015 Int Conf Bio-Med Eng Environm Technol* 164–171
- Lamas WDQ, Palau JCF, De Camargo JR (2013) Waste materials co-processing in cement industry: Ecological efficiency of waste reuse. *Renew Sustain Energy Rev* 19:200–207. <https://doi.org/10.1016/j.rser.2012.11.015>
- Li YL, Zhao XL, Singh Raman RK, Al-Saadi S (2018) Thermal and mechanical properties of alkali-activated slag paste, mortar and concrete utilising seawater and sea sand. *Constr Build Mater* 159:704–724. <https://doi.org/10.1016/j.conbuildmat.2017.10.104>
- Machado G, Santos F, Faria D, De Queiroz TN, Zinani F, De Queiroz JH, Gomes F (2018) Characterization and potential evaluation of residues from the sugarcane industry of Rio Grande do Sul in biorefinery processes. *Nat Resour.* <https://doi.org/10.4236/nr.2018.95011>
- Miranda I, Gominho J, Mirra I, Pereira H (2012) Chemical characterization of barks from *Picea abies* and *Pinus sylvestris* after fractioning into different particle sizes. *Ind Crops Prod* 36:395–400. <https://doi.org/10.1016/j.indcrop.2011.10.035>
- Na B, Wang Z, Wang Z, Ding T, Huang R, Xiaoling L (2014) Study on hydration mechanism of low density magnesia-bonded wood wool panel. *Wood Research* 59(1):137–147
- Olayiwola HO, Amiamdhamen SO, Tyhoda L, Meincken M (2021) Investigating the suitability of fly ash / metakaolin - based geopolymers reinforced with South African alien invasive wood and sugarcane bagasse residues for use in outdoor conditions. *Eur J Wood Prod* 79:611–627. <https://doi.org/10.1007/s00107-020-01636-4>
- Pereira Ferraz G, Frear C, Pelaez-Samaniego MR, Englund K, Garcia-Perez M (2016) Hot water extraction of anaerobic digested dairy fiber for wood plastic composite manufacturing. *BioResources* 11(4):8139–8154. <https://doi.org/10.15376/biores.11.4.8139-8154>
- Petermann JC, Saeed A (2012) Alkali-activated geopolymers: a literature review. Air Force Research Laboratory, Feb 1–99
- Provis JL, Van Deventer JSJ (2014). Alkali Activat Mater. <https://doi.org/10.1007/978-94-007-7672-2>
- Quiroga A, Marzocchi V, Rintoul I (2016) Influence of wood treatments on mechanical properties of wood-cement composites and of *Populus Euroamericana* wood fibers. *Compos B Eng* 84:25–32. <https://doi.org/10.1016/j.compositesb.2015.08.069>
- Rashad AM (2015) Influence of different additives on the properties of sodium sulfate activated slag. *Constr Build Mater* 79:379–389. <https://doi.org/10.1016/j.conbuildmat.2015.01.022>
- Sariatli F (2017) Linear economy versus circular economy: a comparative and analyzer study for optimization of economy for sustainability. *Visegrad J Bioecon Sustain Develop* 6(1):31–34. <https://doi.org/10.1515/vjbsd-2017-0005>
- Shi Z, Shi C, Wan S, Li N, Zhang Z (2018) Effect of alkali dosage and silicate modulus on carbonation of alkali-activated slag mortars. *Cem Concr Res* 113(July):55–64. <https://doi.org/10.1016/j.cemconres.2018.07.005>
- Simatupang MH, Geimer RL (1990) Inorganic binder for wood composites: feasibility and limitations. *Proceedings of Wood Adhesive Symposium*, 169–176. http://www.fpl.fs.fed.us/products/publications/specific_pub.php?posting_id=15141&header_id=p
- Song S, Sohn D, Jennings HM, Mason TO (2000) Hydration of alkali-activated ground granulated blast furnace slag. *J Mater Sci* 35(1):249–257. <https://doi.org/10.1023/A:1004742027117>
- T211 (2012). Ash in wood, pulp, paper and paperboard: combustion at 525°C. Tappi Standards
- Tran DH, Louda P, Bortnovsky O, Bezucha P (2009) Effect of curing temperature on flexural properties of silica-based geopolymer-carbon reinforced composite. *Manuf Eng* 37(2):492–497
- Turku I, KeskiSaari A, Kärki T, Puurtinen A, Marttila P (2016) Characterization of wood plastic composites manufactured from recycled plastic blends. *Compos Struct* 161:469–476. <https://doi.org/10.1016/j.compstruct.2016.11.073>
- Yazdi MA, Liebscher M, Hempel S, Yang J, Mechtcherine V (2018) Correlation of microstructural and mechanical properties of geopolymers produced from fly ash and slag at room temperature. *Constr Build Mater* 191:330–341. <https://doi.org/10.1016/j.conbuildmat.2018.10.037>

Publisher's Note Springer Nature remains neutral with regard to jurisdictional claims in published maps and institutional affiliations.